Optical Receiver Front-end Design Choices to Enhance Throughput of LiFi

X. Liu[1], L. Azarkh[1], J. P. M. G. Linnartz[1,2]

[1]Electrical Engineering, Eindhoven University of Technology, 5600 MB Eindhoven, The Netherlands
[2]Signify (Philips Lighting) Research, 5656 AE Eindhoven, The Netherlands

Abstract

The optical front end (OFE) is a critical part in most Optical Wireless Communication (OWC) systems. It captures the incoming light flux, converts it and amplifies it into an electrical signal. Its photodiode (PD) and transimpedance amplifier (TIA) can limit the throughput, determined by the noise levels and the (gain-) bandwidth. This paper starts with a refined model of the PD and the TIA, in order to analyze in detail the strength and frequency characteristics of the relevant noise sources. At high frequencies signal-to-noise ratio (SNR) degrades due to the capacitance of the PD. This limits the useful modulation bandwidth, though equalization and and frequency–dependent power and bit loading can mitigate this. To some extent, SNR can be traded for bandwidth by choosing an appropriate PD size. We investigate different optical receiver design strategies, where single PD is segmented into pieces, and connected to one or more TIAs. Numerical analysis on channel quality is carried out to compare between various design strategies.

I. Introduction

The increasing demand for wireless data in mobile and Internet-of-Things services puts pressure on the Radio Frequency (RF) spectrum. Optical Wireless Communication (OWC), is drawing great research attention as an alternative to RF in tackling the spectrum congestion challenge. In earlier work we studied limitations caused by the LED [1], where its low-pass frequency characteristics restricts the bandwidth. If increasingly lasers are used, the optical receiver may start to limit performance. In the OFE, which usually consists of a PD and TIA, several noise sources exist. The spectral power density of these noise sources differ [2]. Moreover, these noise contributions are amplified and filtered by the TIA, which changes the output noise spectral power density. Also, the capacitance of the PD significantly influences the signals and noise, particularly at high frequencies [3].

We study various noise sources at the OFE, especially their spectral characteristics and amplification effect of TIA, referenced to the noise input. Together with all the noise sources, an equivalent input noise model with both current and voltage noise sources is built that helps to compute the total output noise power spectral density. Next, we investigate the trade-off of PD capacitance by PD segmentation, in the means of dividing one PD into N pieces, thus decrease the capacitance of each PD. In this case, total output noise spectral density that is amplified by TIA and capacitance of PD is compared between the segmented and non-segmented scenarios. The paper ends with a brief discussion on throughput optimization by means of different modulation strategies based on the channel spectral information, which we will elaborate later. While previous papers describe the impact of the PD area on signal bandwidth, we focus on the impact on the noise.

II. System Description

An OFE with PD and TIA is illustrated in Fig. 1. Photons that arrive at the PD are converted into a current, which is fed into the TIA, which converts it into a voltage

output. R_S, C_S are the parasitic source resistance and capacitance of the PD, which in parallel are responsible for the source impedance $Z_s = R_s||1/j\omega C_S$. The resistor R_F and capacitor C_F of the TIA create the feedback impedance $Z_F = R_F||1/j\omega C_F$.

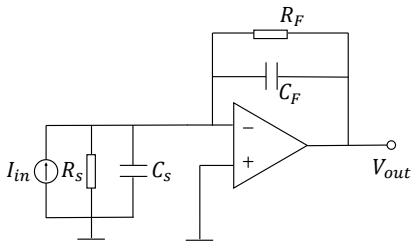

Fig. 1. Optical Receiver Front End

Noise is generated by different sources within the optical receiver front end, from the PD, from the amplifier and from the discrete character of photons. Specifically, five types of input noise sources are identified:

1) Shot noise originates from the statistical nature of light as a statistical arrival of photons. The generated current will also fluctuate with time. It is mostly considered as white noise over the relevant modulation spectrum. However, it is not additive but signal dependent. Its power spectral density is expressed as (q is the electron charge) [4]: $S_{sh}(f) = 2qi_{in}(t)$, where i_{in} denotes the incoming current in time-domain.
2) Dark current noise, which is a relatively small current I_d exists when even no photon is detected by the PD. It is also treated as white and its power spectral density is calculated by [4].
3) Thermal noise for resistors R_F, R_S, generally treated as white noise with power spectral density: $S_{th}(f) = 4kT/R$ where T is the absolute temperature, and k is the Boltzmann's constant.
4) Input current noise of the amplifier. There are number of noise sources in the amplifier. These noise are modelled as an input current and voltage (see below) externally to a noise-free amplifier. The frequency spectrum of the input current noise is colored, where at low frequency it is 1/f noise and white noise at high frequency [5].
5) Input voltage noise of the amplifier. The spectrum is similar to input current noise. The noise power spectral density of the input current and voltage noise is denoted as [5]: $S_{e_{in},i_{in}}(f) = kf_c/f$ where k is the rms input noise power at high frequency, f_c is the corner frequency of the 1/f noise.

The above noise sources are illustrated in Fig. 2. Summing up the input noise, Fig. 3 shows the noise analysis model for the optical receiver front end. i_n includes shot noise, dark current noise, thermal noise, and input current noise of the amplifier. e_n denotes the input voltage noise. The total output noise can be derived via

$$V_{Nout}(f) = G_e(f)e_n(f) + G_i(f)i_n(f) \tag{1}$$

where the amplification of current and voltage noise are

$$G_i(f) = \frac{A(f)Z_F(f)}{1 + A(f)}, G_e(f) = \frac{A(f)}{1 + A(f)\beta(f)} = \frac{A(f)(Z_s + Z_F)}{(Z_s + Z_F) + A(f)Z_s}. \tag{2}$$

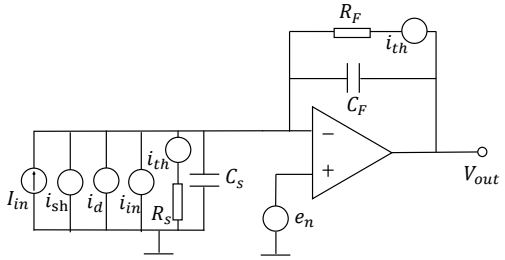

Fig. 2. Noise Sources in OFE

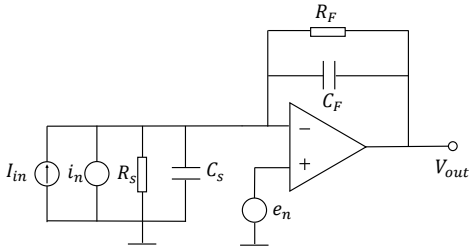

Fig. 3. Noise Model for OFE

where $A(f) = \frac{A_{amp}}{1+f/f_{amp}}$ is the open loop gain for the op-amp, and $\beta = \frac{Z_S}{Z_F+Z_S}$ is the feedback factor of the TIA.

III. PD Segmentation

High capacitance of the PD increases the voltage noise at high frequency because with higher C_S , the voltage noise e_n will be amplified more. As Z_F is fixed, we can expect a degradation of SNR at high frequency. Since the capacitance of PD is in good approximation proportional to the PD area, an effective approach to reduce the noise at high frequency will be to decrease the size of the PD. However, a smaller PD also has a decreased detection area. To maintain a large total detection area while mitigating high frequency noise, one possible solution is to divide the PD into several segments, to connect each segment to its own dedicated TIA, while all the outputs of all amplifiers are summed together.

This section quantifies this effect. One motivation for such study is that as the number of amplifiers increases, more noise contributions will be added. Even if the noise at high frequency is less amplified, the total noise may still be higher than the case without segmentation. In order to address this problem, we consider to use a lens to focus the light on one or several of the PDs, and turn off the receivers with no signal received. Multiple segments are nonetheless needed if the angle of arrival is unknown during design. We consider a number of scenarios for different PD designs:

1) *Single PD* Only one large PD is used, connected with one TIA;
2) *Segmented, non-imaging* The PD is divided into N pieces, each connected to one TIA; All segments receive light, in an equal amount as scenario *Single PD*;
3) *Segmented, imaging*: The PD is segmented similar to scenario 2), but a lens is deployed to focus optical signal to one of the PD segments. PDs and their connected TIAs that do not receive optical power are switched off;

IV. Calculation & Discussion

To quantify the noise levels, we model the op-amp AD8099 with a gain bandwidth = 3.8GHz ($A_{amp} = 85$dB, $f_{amp} = 0.2$MHz), and PD s-5980-10 with source capacitance $C_S = 40/N$ pF and source resistance $R_S = 5M\Omega$. The feedback circuit for TIA is set as $R_F = 1k\Omega$. Fig. 4 shows the noise power spectral density from different noise sources in scenario *Single PD*. Op-amp noise dominates over PD and thermal noise due to the significant amplification of e_n at high frequencies. With the finite gain-bandwidth of op-amp, beyond a certain frequency $f = |Z_S A_{amp} - 1| f_{amp}$ the noise level decreases. Fig. 5 shows the total output noise power spectral density for three PD segmentation

configurations, with segmentation factor $N = 1, 4, 9, 16$. Although *Segmented, non-imaging* shows the highest noise level over the spectrum due to the application of several TIAs, the total noise is less amplified at high frequency compared to *Single PD* since C_S decreases. *Segmented, imaging* has the lowest noise level, since redundant TIAs are switched off as well as the decreased PD capacitance.

In this paper, we did not describe the frequency dependant signal gains, which we include in future work to derive gain-noise ratios and throughput. The frequency characteristics of noise versus size of PD, as addressed here, in combination with signal amplification models give insight in how to design an OFE for best link quality. This allows an optimization of the throughput, for example optimization of OFE design topologies [6], [7], in combination with the modulation scheme including adaptive bandwidths and adaptive bit loading [8]–[10].

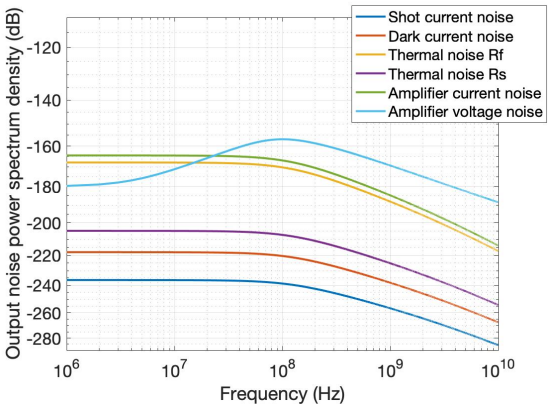

Fig. 4. Output Noise from Different Noise Sources

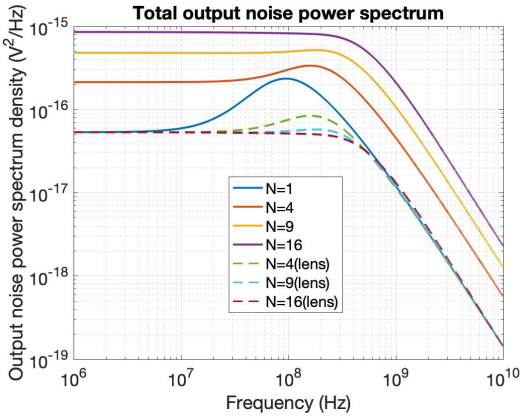

Fig. 5. Total Output Noise Under Different PD Segmentation Scenario

REFERENCES

[1] J.-P. M. G. Linnartz, X. Deng, A. Alexeev, and S. Mardanikorani, "Wireless communication over an led channel," *IEEE Communications Magazine*, vol. 58, no. 12, pp. 77–82, 2020.

[2] *Transimpedance Amplifier Noise Considerations*, Analog Devices, 2002.

[3] G. Royo, A. Martínez-Pérez, C. Sánchcz-Azqueta, C. Aldea, and S. Celma, "Noise reduction technique using multiple photodiodes in optical receivers for pof communications," in *2021 IEEE 12th Latin America Symposium on Circuits and System (LASCAS)*, 2021, pp. 1–4.

[4] R. Hui, *Introduction to fiber-optic communications*. Academic Press, 2019.

[5] B. Carter, "Op amp noise theory and applications," in *Op amps for everyone*. Elsevier, 2009, pp. 163–188.

[6] T. Koonen, K. Mekonnen, F. Huijskens, Z. Cao, and E. Tangdiongga, "Novel broadband owc receiver with large aperture and wide field-of-view," in *2020 European Conference on Optical Communications (ECOC)*, 2020, pp. 1–4.

[7] M. D. Soltani, H. Kazemi, E. Sarbazi, H. Haas, and M. Safari, "Optimal imaging receiver design for high-speed mobile optical wireless communications," in *2022 IEEE International Conference on Communications Workshops (ICC Workshops)*, 2022, pp. 01–06.

[8] T. E. B. Cunha, J.-P. M. G. Linnartz, and X. Deng, "Achievable rate of led-based distributed mimo owc systems under a per-led power constraint," in *2021 17th International Symposium on Wireless Communication Systems (ISWCS)*, 2021, pp. 1–6.

[9] S. Mardanikorani, X. Deng, and J.-P. M. G. Linnartz, "Optimization and comparison of m-pam and optical ofdm modulation for optical wireless communication," *IEEE Open Journal of the Communications Society*, vol. 1, pp. 1721–1737, 2020.

[10] ——, "Sub-carrier loading strategies for dco-ofdm led communication," *IEEE Transactions on Communications*, vol. 68, no. 2, pp. 1101–1117, 2020.